16th World Conference on Earthquake, 16WCEE 2017
Santiago Chile, January 9th to 13th 2017
Paper N° 198 (Abstract ID)
Registration Code: S-H1461229905

EFFECTS OF PERMANENT OFFSET ON THE RESPONSE OF THE CURVED SURFACE SLIDERS

P. Dubini(1), V. Quaglini(2), E. Gandelli(3)

(1) *Research Fellow, Politecnico di Milano, Piazza Leonardo da Vinci 32 – 20133 Milano – Italy, paolo.dubini@polimi.it*
(2) *Associate Professor, Politecnico di Milano, Piazza Leonardo da Vinci 32 – 20133 Milano – Italy, virginio.quaglini@polimi.it*
(3) *PhD Student, Politecnico di Milano, Piazza Leonardo da Vinci 32 – 20133 Milano – Italy, emanuele.gandelli@polimi.it*

Abstract

The large worldwide diffusion of isolation systems with Curved Surface Sliders (CSS), also known as the Friction Pendulum System®, requires detailed knowledge of their behavior and improved modelling capability under seismic conditions. Restoring capability after the earthquake is one of the fundamental functions required to seismic isolation systems. It is noted the dependency of residual displacements on ground motions characteristics and isolator mechanical properties, namely the radius of curvature and the coefficient of friction. Current standards on antiseismic devices (EN15129, AASHTO) and design codes (Eurocode 8) provide criteria to ensure good restoring capability. An analytical model has also been formulated based on numerical analysis to predict the residual displacement of the isolation system. In mainshock-aftershock sequences it is possible that at the occurrence of the aftershock the isolation system present an offset from its original configuration as a result of the main shock. The main concern is whether or not an increase in the maximum or residual displacement consequent to the displacement accrual starting from the offset position may lead, under certain conditions, to exceed the displacement capacity of CSS device and the structural integrity or compromise the serviceability of the structure. In this study, some hundreds of nonlinear time-history analyses of SDOF systems were conducted within an extensive parametric study aimed to investigate the effects of a non-centered initial position on the CSS response, in terms of maximum and residual displacements. Five different initial offsets were considered coupled with a wide range of devices and earthquakes, characterized by different values of the isolator design parameters and characteristics of the ground motion. Twenty different CCS isolators were considered varying five radii of curvature (from 2 200 mm to 5 000 mm) and four friction laws, covering the current design practice. Twenty-four natural ground motion time histories were selected from a database and classified in terms of the predominant period of the quake and the level of impulsivity (to this scope, a "Pulse Index" was formulated based on the rate of transmission of the kinetic energy). The effects of an initial offset are discussed herein in terms of maximum and residual displacements of the isolators. The displacement responses obtained in presence of the offset are eventually compared with the relevant response provided by the isolation system that moves from its centred configuration.

Keywords: Curved Surface Slider, re-centering, parametric study

1. Introduction

The re-centring capability, i.e. the ability to return towards the origin at the end of a ground motion, is recognized by the current European seismic code, or Eurocode 8 [1, 2], as one of the four fundamental functions of base isolation systems. This capability is associated with the fulfilment of the fundamental requirements for structures in seismic areas, i.e. the damage limitation and the no-collapse requirement, as substantial residual displacement after the earthquake may affect the serviceability of the structure and possibly jeopardize the functionality of lifelines and non structural elements crossing the isolation plane (such as fire protection and weather proofing elements, elevators, etc.), and eventually limit the capability of the isolation system to withstand future earthquakes. The re-centering capability assumes a primary importance due to the significant field evidence of seismic sequences characterized by frequent medium-strong intensity ground motions following a strong mainshock after short intervals of time, as recorded also in recent earthquakes [3-8]. Since it may not be possible to re-center the system before the occurrence of close aftershocks, a concern is related to the possibility that ground motion sequences with such characteristics would entail an accrual of displacements, and the deformation capacity of the isolation system designed on the basis of a single earthquake possibly becomes inadequate at the end of the seismic sequence.
According to the provisions of the Eurocode 8, an isolation system is deemed to have sufficient self-centring capability in one horizontal direction when the condition is met.

$$\frac{d_{\mathrm{m}}}{d_{rm}} \geq \delta \tag{1}$$

where d_m is the maximum design displacement of the isolation system in the examined direction, d_{rm} is the maximum residual displacement for which the isolating system can be in static equilibrium in the considered direction, i.e. the residual displacement under which the static equilibrium is reached at unloading from d_m under quasi-static conditions, and δ is a numeric coefficient, whose recommended value is 0.5. For an isolation system with bilinear hysteretic behaviour the maximum residual displacement d_{rm} is given by the ratio between the characteristic strength F_0 and the restoring stiffness K_P (Fig.1) and depends only on the fundamental mechanical characteristic of the system, whereas d_m depends also on the details of the seismic ground motion.

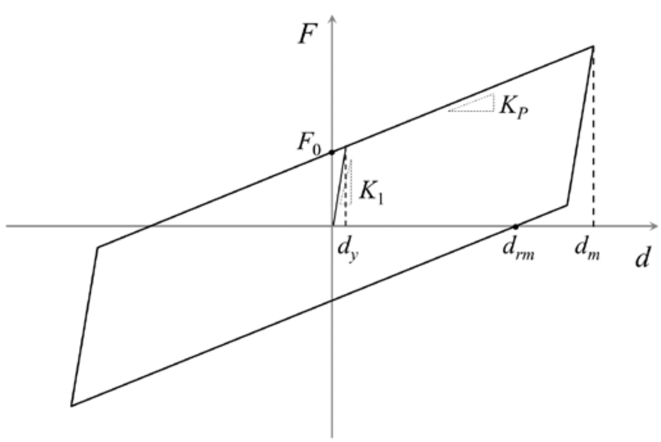

Fig. 1 – Force – displacement characteristic of a bilinear hysteretic isolation system

The Eurocode recommends that systems which do not satisfy the re-centring provision of Eq. (1) in a certain direction have sufficient displacement capacity in order to accommodate, with adequate reliability, the accumulation of residual displacements in this direction during the service life of the structure. The code hence provides a formula for estimating the necessary increase in the displacement capacity to account for the build-up of residual displacements under a sequence of earthquake events occurring before the design earthquake, considered to have a collective probability equal to the probability of the design earthquake. The maximum displacement that can be accommodated by the system must be increased by a factor

$$\rho_d = 1 + 1.35 \frac{1 - \left(d_y / d_m\right)^{0.6}}{1 + 80\left(d_m / d_{rm}\right)^{1.5}} \tag{2}$$

where d_y is the yield displacement of the equivalent bilinear system (see Fig.1). For systems with d_m / d_{rm} > 0.5 the effect of the accumulation of residual displacements is insignificant (ρ_d < 1.05).
Katsaras et al. [9] examined the validity of the re-centring criterion (Eq. (1)) in a parametric study, analysing 150 different combinations of system parameters and 122 natural ground motions, and concluded that bilinear hysteretic isolation systems with d_m / $d_{rm} \geq 0.5$ have small residual displacements compared with the maximum displacement produced by the ground motion, and insignificant accumulation of residual displacements at the end of a sequence of earthquakes. This conclusion is in line with the results of an experimental study on isolation systems for bridges comprised of flat sliding bearings, rubber devices and fluid dampers [10] which showed that the system exhibits strong re-centring capability when the ratio of its characteristic strength F_0 to the peak restoring force at the maximum displacement d_m, i.e. K_P d_m , is less than or equal to 3, which corresponds to d_m / d_{rm} > 0.33. Another parametric study pointed that the Eurocode provision (Eq. (1)) is valid for isolation systems with "flag-shaped" force – displacement characteristic, such as systems comprising self-centring elements made of Shape Memory Alloys, when δ is assumed as large as 3 [11].
A re-centring criterion based on energy concepts is provided in the European standard on antiseismic devices [12]. This criterion states that the isolation system has sufficient re-centring capability when

$$E_S \geq 0.25 \; E_H \tag{3}$$

where E_S is the reversibly stored energy and E_H is the energy dissipated in hysteretic deformation when the system moves from its origin to the position of maximum displacement. For bilinear hysteretic systems the provisions given in Eq. (1) and (3) are equivalent when δ = 0.5 [13].
The restoring behaviour of Curved Surface Sliders is noted to depend on both the mechanical properties of the isolator and the details of the ground motion time history [14].
A parametric study is performed and the properties of the CSS are varied to cover the typical production ranges of current manufacturers, whereas a set of natural ground motions with different frequency contents is selected for the analyses.
Since the current practice in isolated structure modelling consider the CCS starting from a centred configuration, the aim of the study is to investigate the effect of an initial offset on the maximum and residual displacement of the CSS isolation system during an earthquake. An increase in the maximum displacement, consequent to an initial offset, may lead to exceed the displacement capacity of CSS and to compromise the structural integrity; an accrual of residual displacement may also affect the serviceability of the structure.
An artificial offset determined as the residual displacement occurring when the system is released from an extreme position corresponding to its reference displacement capacity [14] is applied to the isolation system and the CSS response in terms of maximum and residual displacement in presence of such offset is eventually compared with the response provided by the isolation system when it moves from its centred configuration.
The results are also compared with EC8 Eq. (2) for the estimation of the necessary increase in the displacement capacity to account for the build-up of residual displacements.

2. Numerical Analysis

Some hundreds of nonlinear response history analyses of SDOF systems were carried on within an extensive parametric study aimed to investigate the effects of a non-centered initial position on the CSS response, in terms of maximum and residual displacements. A mass of 100 tons, typical of medium-rise residential buildings [14], was considered.

The seismic input consisted of one-directional horizontal ground motion time histories, whereas the vertical component of the seismic excitation was not taken into account.

The numerical model was implemented in the structural analysis program OPENSEES v.2.5.4 [15], using a nonlinear "friction bearing" element to model the hysteretic behaviour of the isolation system. The velocity dependent friction model is described by the equation [16]:

$$\mu = \mu_{\mathrm{LV}} - (\mu_{\mathrm{HV}} - \mu_{\mathrm{LV}}) \cdot \exp(-\alpha \cdot |V|) \tag{4}$$

where μ_{LV} and μ_{HV} are two parameters that represent the coefficient of friction at very low and very high velocity, respectively, and α is a parameter that describes the rate of transition from μ_{LV} to μ_{HV}. The restoring stiffness of the isolation system was defined as $K_P = W/R$, where W is the vertical load acting though the isolation system, and R is the radius of curvature of the CSS. Finally, an initial stiffness $K_1 = 100\ K_P$ was assumed in order to minimize the elastic deformation.

2.1 Parameters of Curved Surface Sliders

Twenty different CCS isolators were considered varying five radii of curvature R (2 200 , 3 000 , 3 500 , 4 000 , 5 000 mm) and four friction laws (f2, f3, f4, f5), covering the current design practice in the European market (Table 1). The undamped vibration periods $T_{is} = 2\pi\sqrt{\frac{R}{g}}$ of the considered CSS span from 2 to 4 seconds.

The high velocity friction coefficient μ_{HV} ranged between 5% and 12.5%, with 2.5% step; the ratio $\mu_{\mathrm{HV}}/\mu_{\mathrm{LV}}$ = 2.5 was assumed and the transition rate was set to α = 0.0055 s/mm, in accordance with [14]. Although the analysis did not directly consider the effects of normal load and air-temperature variations on the coefficient of friction of the sliding surfaces [17, 18], they are assumed to be indirectly covered by the range of the friction coefficient.

Table 1 – CSS parameters examined in the study

parameter	**values**	**number of cases**
radius, R	2 200 , 3 000 , 3 500 , 4 000 , 5 000 mm	5
coefficient of friction, μ	f2 (μ_{LV} = 0.020 ; μ_{HV} = 0.050 ; α = 0.0055 s/mm) f3 (μ_{LV} = 0.030 ; μ_{HV} = 0.075 ; α = 0.0055 s/mm) f4 (μ_{LV} = 0.040 ; μ_{HV} = 0.100 ; α = 0.0055 s/mm) f5 (μ_{LV} = 0.050 ; μ_{HV} = 0.125 ; α = 0.0055 s/mm)	4

In order to avoid extreme vertical displacements, the horizontal displacement capacity of the CSS is limited from the radius of curvature. According to this practice, in the study a reference displacement capacity equal to d_c = 0.2 R was assumed [19].

2.2 Seismic input classification

To investigate a variety of ground motions with different frequency content, the Pacific Earthquake Engineering Research Center (PEER) database (http://peer.berkeley.edu/nga) was categorized based on its pulse-like characteristic and the period T_{sv} at the maximum level of the undamped velocity response spectrum.

In this study a "Pulse Index" was proposed for classification of pulse-like records. The pulse index PI_k is defined as the ratio between the time interval $D_{v,T}$ during which the most of the seismic energy is introduced in the structure, and the duration of the quake $D_{v,B}$

$$PI_k = 1 - \frac{D_{v,T}}{D_{v,B}} \tag{5}$$

where $D_{v,T}$ and $D_{v,B}$ are the Trifunac [20] and the bracketed [21] durations of the ground motion, respectively. $D_{v,T}$ is calculated as the length of time between the instants when the 5% and the 95% of the energy integral $I_E = \int_0^\infty v_g^2 dt$ [22] is developed

$$D_{v,T} = t_{0.95\,I_E} - t_{0.05\,I_E} \tag{6}$$

and $D_{v,B}$ is the total time between the first and the last exceeding of a given threshold during the strong motion. Here the threshold has been fixed at 1% of the absolute peak velocity.

The pulse-like characteristic of the ground motion was ranked depending on the PI_k value into three categories:

- no pulse $PI_k < 0.40$
- weakly pulse $0.40 \leq PI_k \leq 0.70$
- pulse-like $PI_k > 0.70$

Four ranges of T_{sv} were established, corresponding to the natural periods of the isolation systems according to Table 1

- $T_{sv} \leq 2.0$ sec
- $2.0 < T_{sv} \leq 3.0$ sec
- $3.0 < T_{sv} \leq 4.0$ sec
- $T_{sv} > 4.0$ sec

For pulse-like seismic ground motions, T_{sv} coincides with the so-called “pulse period” T_p, corresponding to the dominant peak of the velocity response spectrum at which the largest quantity of seismic energy is available. For no pulse ground motions significant energy content can be available over a range around T_{sv} depending on the smoothness of the spectrum.

2.3 Selected events

Twenty-four natural ground motion time histories were selected from the Pacific Earthquake Engineering Research Center (PEER) (Table 2). The records were selected with lowest usable frequency (l.u.f.) [23] less than 0.2 Hz accounting for the undamped vibration frequency of the considered CSS isolators. Though not exhaustive, the set spans the possible ranges of pulsativity and frequency content of interest for base isolation.

The acceleration time histories were scaled in order to produce displacement of the isolation system of practical interest (i.e. maximum displacement d_m at least 20% of the reference displacement capacity d_c), but the seismic records do not need to be compatible with any reference response spectrum, as aftershocks may occur at any seismic intensity. Even better, the selected seismic records should generate a great variety of peak displacement values, in order to really investigate the effect of the initial offset on the probability of increase of d_m.

Table 2 – Selected seismic ground motion records

T_{sv} range	Type	Event	PEER file	T_{sv} (s)	PI_k (-)	*l.u.f.* (Hz)	*S.F.* (-)	*PGA* (g)
$T_{sv} \leq 2$ s	no pulse	Chi-Chi, 1999	RSN3860_CHICHI.05_CHY008N	0.37	0.33	0.075	4.7	0.6
		Chi-Chi, 1999	RSN3858_CHICHI.05_CHY004N	0.34	0.38	0.075	10.4	0.6
	weakly pulse	Nahanni, 1985	RSN496_NAHANNI_S2330	0.52	0.56	0.125	1.9	0.6
		Chi-Chi, 1999	RSN3846_CHICHI.03_CHY008W	1.52	0.55	0.063	9.9	0.3
	pulse-like	Morgan Hill 1984	RSN451_MORGAN_CYC285	0.83	0.86	0.125	0.5	0.6
		Coyote Lake, 1979	RSN150_COYOTELK_G06230	1.47	0.84	0.075	1.4	0.6
$2 < T_{sv} \leq 3$ s	no pulse	Chi-Chi, 1999	RSN2938_CHICHI.05_CHY016N	2.34	0.29	0.075	10.7	0.5
		Chi-Chi, 1999	RSN3844_CHICHI.03_CHY004N	2.69	0.34	0.038	7.7	0.5
	weakly pulse	Cape Mendocino, 1992	RSN827_CAPEMEND_FOR000	2.56	0.51	0.070	2.6	0.3
		Chi-Chi, 1999	RSN3844_CHICHI.03_CHY004W	2.90	0.59	0.038	5.6	0.3
	pulse-like	Irpinia, 1980	RSN292_ITALY_A-STU270	2.82	0.82	0.125	0.8	0.3
		Imperial Valley, 1979	RSN171_IMPVALL.H_H-EMO270	2.94	0.85	0.100	1.0	0.3
$3 < T_{sv} \leq 4$ s	no pulse	Alaska, 2002	RSN2102_DENALI_NOAA-90	3.43	0.24	0.026	21.4	0.3
		Irpinia Eq, 1980	RSN297_ITALY_B-BIS270.	3.83	0.39	0.163	7.0	0.5
	weakly pulse	Cape Mendocino, 1992	RSN827_CAPEMEND_FOR090	3.08	0.46	0.070	2.7	0.3
		Chi-Chi, 1999	RSN2695_CHICHI.04_CHY016W	3.82	0.48	0.050	13.3	0.5
	pulse-like	Imperial Valley, 1979	RSN181_IMPVALL.H_H-E06230	3.40	0.89	0.063	0.6	0.25
		Imperial Valley, 1979	RSN182_IMPVALL.H_H-E07230	3.27	0.85	0.075	1.1	0.5
$T_{sv} > 4$ s	no pulse	Chi-Chi, 1999	RSN3851_CHICHI.04_CHY004W	5.07	0.36	0.100	14.0	0.3
		Landers, 1992	RSN834_LANDERS_ARC262	5.05	0.35	0.017	11.0	0.3
	weakly pulse	Alaska, 2002	RSN2115_DENALI_PS11-66	5.76	0.47	0.130	8.3	0.6
		Kocaeli, 1999	RSN1170_KOCAELI_MCD090	5.88	0.59	0.075	8.8	0.6
	pulse-like	Kocaeli, 1999	RSN1148_KOCAELI_ARE090	5.31	0.70	0.088	2.0	0.3
		Imperial Valley, 1979	RSN179_IMPVALL.H_H-E04230	4.08	0.76	0.063	0.8	0.3

S.F., Scale Factor ; *PGA*, Peak Ground Acceleration (scaled)

2.4 Initial offset estimation

For a medium rise building like the one considered in the study, the temperature induced displacements can be deemed to be small in comparison to permanent displacements produced by other effects, and the possible offset of the isolation system is assumed to correspond to the residual displacement occurring after the system is displaced to a deformed configuration and then released.

Hence in the study the artificial initial offset was evaluated through the 90th percentile equation (Eq. (7)) propose by Cardone et al. [14], defined as the maximum residual displacement resulting from a horizontal deformation to the reference displacement capacity d_c.

For the Curved Surface Slider system the 90th percentile residual displacement $d_{r,90\%}$ is related to the peak displacement d_m by the regression equation

$$d_{r,90\%} = 0.18 \cdot d_m \cdot \left(\frac{d_m}{d_{rm}} \right)^{-0.57} \tag{7}$$

where d_{rm} is the static residual displacement, expressed as the product of the friction coefficient at low velocity and the radius of curvature [24]

$$d_{rm} = \mu_{LV} \cdot R \tag{8}$$

The maximum initial offset was estimated for every combination of radius and coefficient of friction in accordance with Table 1, by assuming that the isolators are displaced to the maximum possible displacement capacity that they are designed to accommodate, i.e. by setting $d_m = d_c$ in Eq. (1).

In this way the maximum offset considered in the analyses is directly related to the mechanical properties of the Curved Surface Sliders (Table 3) and independent of the actual seismic scenario within all the possible scenarios covered by the displacement capacity of the isolation system.

Table 3 – The 90th percentile residual displacement based on reference displacement capacity of the isolation system

R **(mm)**	d_c **(mm)**	**coefficient of friction** μ	d_{rm} **(mm)**	$d_{r,90\%} / d_o$ **(mm)**
2 200	440	f2	44	21.3
		f3	66	26.9
		f4	88	31.6
		f5	110	35.9
3 000	660	f2	60	29.1
		f3	90	36.6
		f4	120	43.2
		f5	150	49.0
3 500	700	f2	70	33.9
		f3	105	42.7
		f4	140	50.3
		f5	175	57.2
4 000	800	f2	80	38.8
		f3	120	48.8
		f4	160	57.5
		f5	200	65.3
5 000	1000	f2	100	48.4
		f3	150	61.0
		f4	200	71.9
		f5	250	81.7

For every combination of mechanical parameters in accordance with Table 1, and every ground motion record (Table 2), five non linear history analyses were conducted, considering five different values of the displacement offset d_o, namely d_o = +1.0$d_{r,90\%}$, +0.5$d_{r,90\%}$, 0 , -0.5$d_{r,90\%}$, -1.0$d_{r,90\%}$.

In order to evaluate possible directionality effects of the selected ground motion time histories, the offset was imposed in either direction of longitudinal displacement. A total number of 2 400 analyses was performed.

3. Results

The response parameters considered hereinafter are introduced in Fig.2: $d_{m,o}$ and d_m are the maximum displacement of the isolation system either from an initial offset d_o, or from the centered position respectively, whereas $d_{r,o}$ and d_r denote the corresponding residual displacements. The results of the analyses are summarized in Fig. 3 to 6:

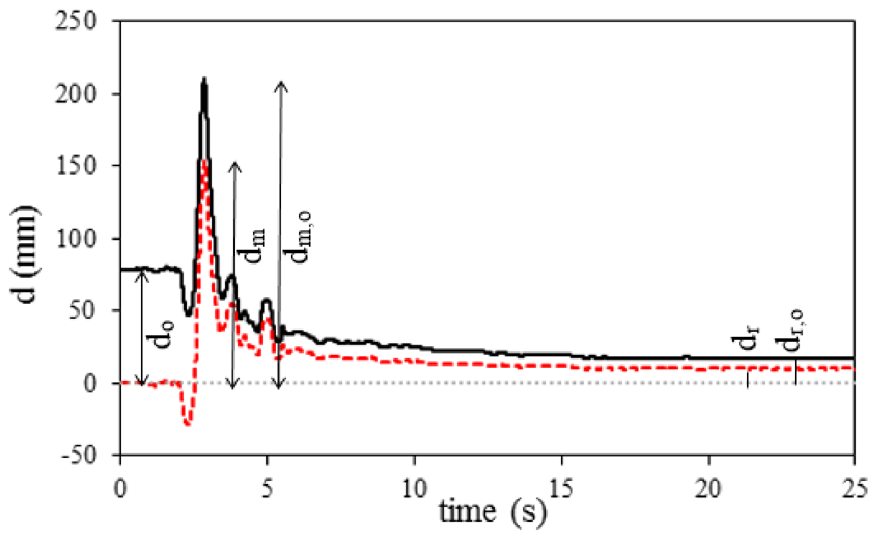

Fig. 2 – Time-histories displacement response parameters of the isolated structure with initial offset (solid black line) and without initial offset (dotted red line)

To preserve the structural integrity of the base-isolated structures during the seismic shaking the maximum displacement must not exceed the capacity of the isolators.

A quantification of the influence of the initial offset on the extreme movement is given in Fig.3, where the relative change of the peak displacement following the initial offset, $d_{m,o}$ / d_m, is plot as a function of the ratio d_m / d_{rm} between the displacement demand of the isolation system with no offset and the static residual displacement (see Eq. (2)).

It is evident from Fig.3, left that the larger the offset d_o, the higher the influence on the maximum displacement (which can result either in an amplification $d_{m,o} / d_m > 1$ or a decrease $d_{m,o} / d_m < 1$). A regression analysis has been performed to determine the curve enveloping the 90th percentile (Fig.3, right):

(a) for $d_m / d_{rm} \leq 0.5$, the ratio $d_{m,o} / d_m$ can be as high as 2 or more with an initial offset $d_o = |1.0\ d_{r,90\%}|$ and as high as 1.5 with an initial offset $d_o = |0.5\ d_{r,90\%}\ |$; however depending on the ground motion characteristics the offset can have the opposite effect of reducing the peak displacement ($d_{m,o} / d_m < 1$);

(b) for $0.5 < d_m / d_{rm} \leq 1.0$, the effect of the offset is smaller ($d_{m,o} / d_m < 1.5$) but not yet negligible; values of $d_{m,o}$ / d_m less than unity are possible as well;

(c) for $d_m / d_{rm} > 1.0$, the effect of the offset is virtually negligible.

In comparison with the formula recommended in the EC 8 (Eq. (2)) for estimating the increase of maximum displacement in case of insufficient re-centring capability, the results of the numerical analyses provide a substantially higher value of $d_{m,o} / d_m$ when $d_m / d_{rm} < 1$ while the difference becomes insignificant when d_m / $d_{rm} > 1.2$.

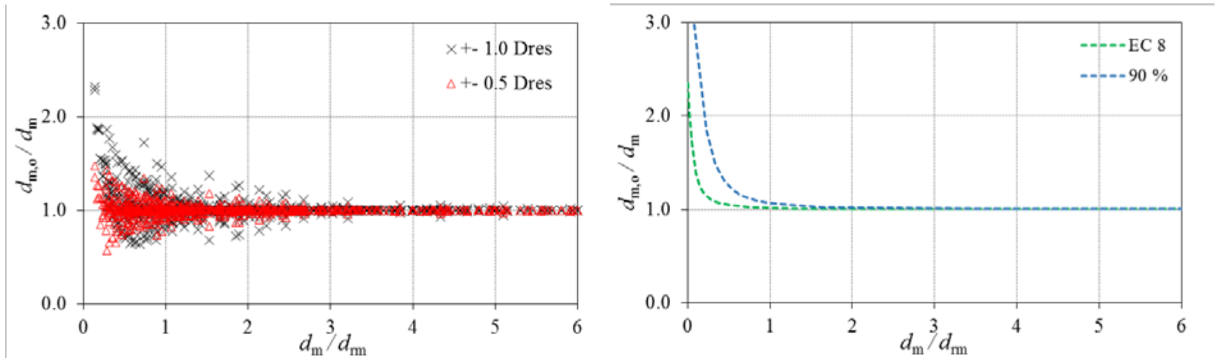

Fig. 3 – Influence of the initial offset on the maximum displacement increase (left) and comparison (at 90% percentile) with EC 8 (right)

The sensitivity of $d_{m,o}$ / d_m on the friction and the radius of curvature of the Curved Surface Slider are shown in Fig.4a and Fig.4b respectively. As predictable, devices with large friction (f4 and f5) and large radius (4 500 mm and 5 000 mm) are more sensitive to the initial offset because characterized by less re-centring capability (large d_{rm}); indeed the largest number of analyses showing significant displacement increase are related to such devices. Conversely, values of $d_{m,o}$ / d_m close to unity mainly occur for isolators with low friction (f2 and f3) and/or low radius of curvature (2 200 mm, 3 000 mm, and 3 500 mm).

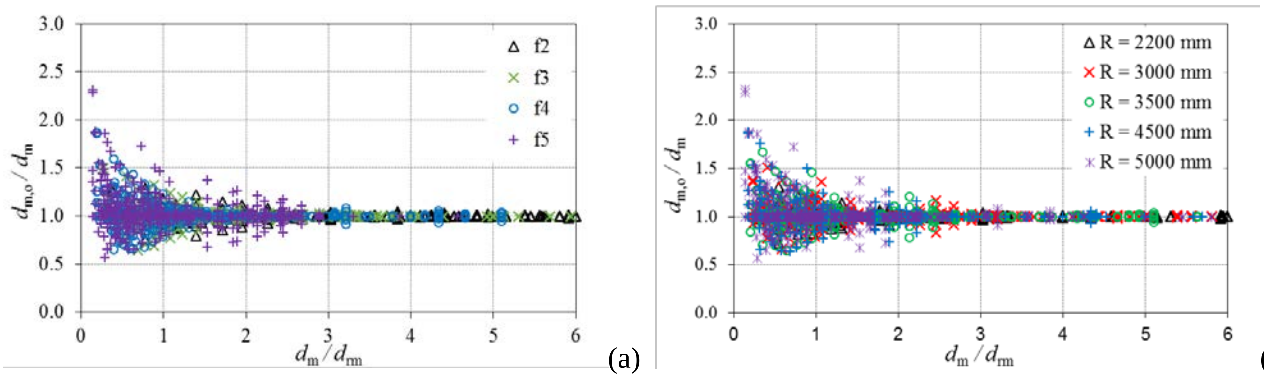

Fig. 4 – Influence of the initial offset on the maximum displacement: dependence on the friction (a), on the radius of curvature of the CSS isolator (b)

Another concern, related to the minimization of damage of base-isolated structures, is the possible accrual of residual displacements during sequences of seismic shakes. Fig.5 compares the residual displacements $d_{r,o}$ and d_r of the isolation system calculated either with or without consideration of an initial offset d_o representing the effect of the previous history. Both $d_{r,o}$ and d_r are normalized to the radius of curvature R of the slider. In the pictures, data points located above the bisector of the quadrant correspond to an accrual of residual displacement; on the contrary, points located below the bisector correspond to a reduction. As shown in Fig. 5a and 5b, the influence of the initial offset on the residual displacement is evident only for CSS isolator with large friction and radius.

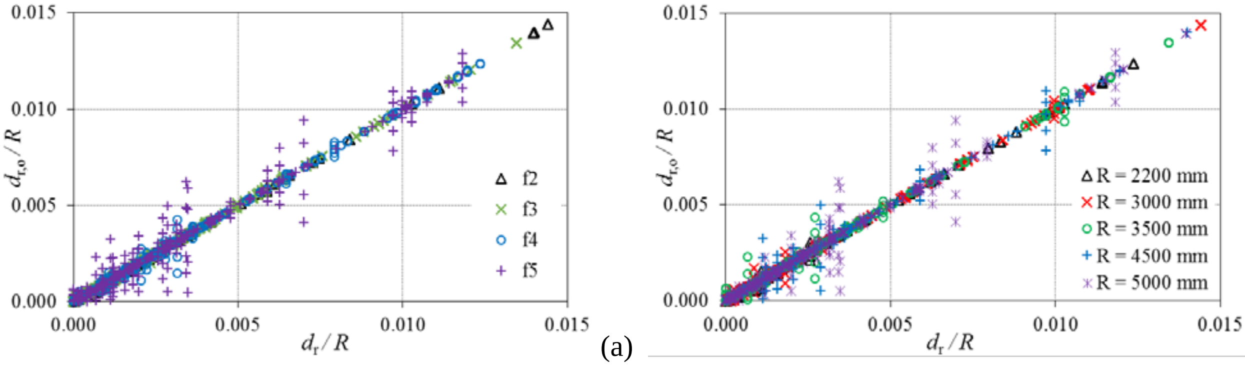

Fig. 5 – Influence of the initial offset on the residual displacement: dependence on the friction (a), on the radius of curvature of the CSS isolator (b)

The effect of the initial offset on the re-centring capability of CSS isolators, has been investigated in Fig.6, where the ratio $d_{r,o}$ / d_m is shown as a function of d_m / d_{rm} . The curve corresponding to the 90th percentile of the responses of isolation systems with the initial offset is shown (Fig.6).

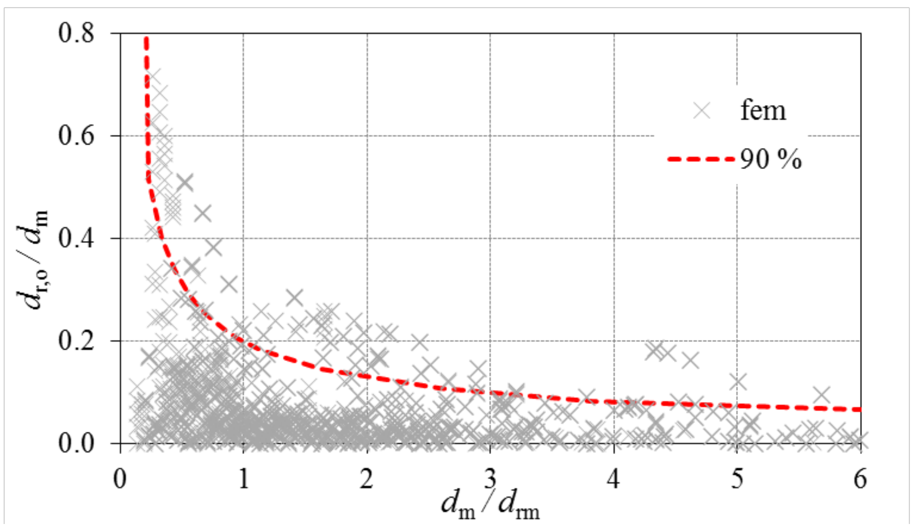

Fig. 6 – Influence of the initial offset on the re-centring capability and the 90th percentile of non linear response analysis results

4. Conclusions

The effect of an initial offset on the displacement response of an isolation system made of Curved Surface Sliders to a ground motion has been investigated in a parametric study. The mechanical properties of the CSS has been varied to cover the typical ranges of current manufacturers, whereas a set of natural ground motions has been selected for the analyses. The main outcomes are summarized in the next points.

(1) the larger the offset d_o, the higher the influence on the maximum displacement (which can result either in an amplification $d_{m,o}$ / d_m > 1 or a decrease $d_{m,o}$ / d_m < 1);

(2) devices with large friction (f4 and f5) and large radius (4 500 mm and 5 000 mm) are more sensitive to the initial offset either in terms of maximum displacement and of residual displacement;

(3) compared with the formula recommended in the EC 8 (Eq. (2)) for estimating the possible increase of maximum displacement in case of insufficient re-centring capability, the results of the numerical analyses

provide a substantially higher value of $d_{m,o}$ / d_m when d_m / d_{rm} < 1 while the difference becomes insignificant when d_m / d_{rm} > 1.2.

5. References

[1] CEN Eurocode 8: design of structures for earthquake resistance—Part 1: General rules, seismic actions and rules for buildings, EN1998-1:2004. European Committee for Standardization, Bruxelles, Belgium, 2004.

[2] CEN Eurocode 8: design of structures for earthquake resistance—Part 2: Bridges, EN1998-2:2005+A1:2011. European Committee for Standardization, Bruxelles, Belgium, 2005.

[3] Decanini L, Gavarini C, Mollaioli F (2000): Some remarks on the Umbria-Marche earthquakes of 1997. *European Earthquake Engineering*, **3**, 18-48.

[4] Huang Y, Wu JP, Zhang TZ, Zhang DN (2008): Relocation of the M 8.0 Wenchuan earthquake and its aftershock sequence. *Science in China (Series D)*, **51** (12), 1703–1711, DOI: 10.1007/s11430-008-0135-z.

[5] Di Sarno L, Elnashai AS, Manfredi G. (2011): Assessment of RC columns subjected to horizontal and vertical ground motions recorded during the 2009 L'Aquila (Italy) earthquake. *Engineering Structures*, **33** (5), 1514-1535, DOI:10.1016/j.engstruct.2011.01.023.

[6] Di Sarno L, Yenidogan C, Erdik M (2013): Field evidence and numerical investigation of the Mw = 7.1 October 23 Van, Tabanli and the Mw > 5.7 November Earthquakes of 2011. *Bulletin of Earthquake Engineering*, **11** (1), 313-346, DOI: 10.1007/s10518-012-9417-0.

[7] Motosaka M, Mitsuji K (2012): Building damage during the 2011 off the Pacific coast of Tohoku Earthquake. *Soils and Foundations* **52** (5), 929-944, DOI:10.1016/j.sandf.2012.11.012.

[8] Carydis P, Castiglioni C, Lekkas E, Kostaki I, Lebesis N, Drei A (2012): The Emilia Romagna, May 2012 earthquake sequence. The influence of the vertical earthquake component and related geoscientific and engineering aspects. *Ingegneria Sismica – International Journal of Earthquake Engineering*, **XXIX**, 31-58.

[9] Katsaras CP, Panagiotakos TB, Kolias B (2008): Restoring capability of bilinear hysteretic seismic isolation systems. *Earthquake Engineering and Structural Dynamics*, **37** (4), 557-575, DOI: 10.1002/eqe.772.

[10] Tsopelas P, Constantinou MC (1994): NCEER - TAISEI corporation research program on sliding seismic isolation systems for bridges - experimental and analytical study of a system consisting of sliding bearings and fluid restoring force/damping devices. *Technical Report NCEER-94-0014*, National Center for Earthquake Engineering Research, Buffalo, USA.

[11] Cardone D (2012): Re-centering capability of flag-shaped seismic isolation systems. *Bulletin of Earthquake Engineering*, **10** (4), 1267–1284, DOI 10.1007/s10518-012-9343-1.

[12] CEN EN 15129: Anti-Seismic Devices. European Committee for Standardization, Bruxelles, Belgium, 2009.

[13] Medeot R (2004): Re-centring capability evaluation of seismic isolation systems based on energy concepts. *Proceedings of the 13th World Conference on Earthquake Engineering*, paper 3106, Vancouver, Canada.

[14] Cardone D, Gesualdi G, Brancato P (2015): Restoring capability of friction pendulum seismic isolation systems. *Bulletin of Earthquake Engineering*, **13** (8), 2449-2480, DOI: 10.1007/s10518-014-9719-5.

[15] McKenna F, Fenves GL, Scott MH, Jeremic B (2000): Open System for Earthquake Engineering Simulation (OpenSees). Pacific Earthquake Engineering Research Center (PEER), Berkeley, USA.

[16] Constantinou MC, Mokha A, Reinhorn AM (1991): Teflon bearings in base isolation. II: modeling. *Journal of Structural Engineering*, **116** (2), 455–474, DOI: 10.1061/(ASCE)0733-9445(1990)116:2(455).

[17] Dolce M, Cardone D, Croatto F (2005): Frictional behaviour of steel-PTFE interfaces for seismic isolation. *Bulletin of Earthquake Engineering*, **3** (1), 75-99, DOI: 10.1007/s10518-005-0187-9.

[18] Quaglini V, Dubini P, Poggi C (2012): Experimental assessment of sliding materials for seismic isolation systems. *Bulletin of Earthquake Engineering*, **10** (2), 717–740, DOI: 10.1007/s10518-011-9308-9.

[19] Calvi GM, Pietra D, Moratti M (2010): Criteri per la progettazione di dispositivi di isolamento a pendolo scorrevole. *Progettazione Sismica*, **3** (1), 7-30.

[20] Trifunac MD, Brady AG (1975): A study of duration of strong earthquake ground motion. *Bulletin of the Seismological Society of America*, **65** (3), 581-626.

[21] Bolt BA (1969): Duration of strong motion. *Proceedings of the 4th World Conference on Earthquake Engineering*, Santiago, Chile.

[22] Anderson JC, Bertero VV (1987): Uncertainties in establishing design earthquakes. *Journal of Structural Eng ineering*, **113** (8), 1709–1724.

[23] Ancheta TD, Darragh RB, Stewart JP, Seyhan E, Silva WJ, Chiou BSJ, Wooddell KE, Graves RW, Kottke AR, Boore DM, Kishida T, Donahue JL (2013): PEER NGA-West2 Database, PEER 2013/03. Pacific Earthquake Engineering Research Center (PEER), Berkeley, USA.

[24] Quaglini V, Gandelli E, Dubini P (2016): Experimental investigation of re-centring capability of curved surface sliders. *Structural Control and Health Monitoring*, published online, DOI: 10.1002/stc.1870.